

REPORT

An early transition state for folding of the P4-P6 RNA domain

SCOTT K. SILVERMAN^{1,3} and THOMAS R. CECH^{1,2}

¹Department of Chemistry and Biochemistry, University of Colorado at Boulder, Boulder, Colorado 80309-0215, USA

²Howard Hughes Medical Institute, University of Colorado at Boulder, Boulder, Colorado 80309-0215, USA

ABSTRACT

Tertiary folding of the 160-nt P4-P6 domain of the *Tetrahymena* group I intron RNA involves burying of substantial surface area, providing a model for the folding of other large RNA domains involved in catalysis. Stopped-flow fluorescence was used to monitor the Mg²⁺-induced tertiary folding of pyrene-labeled P4-P6. At 35 °C with [Mg²⁺] ≈ 10 mM, P4-P6 folds on the tens of milliseconds timescale with $k_{obs} = 15\text{--}31\text{ s}^{-1}$. From these values, an activation free energy ΔG^\ddagger of ~8–16 kcal/mol is calculated, where the large range for ΔG^\ddagger arises from uncertainty in the pre-exponential factor relating k_{obs} and ΔG^\ddagger . The folding rates of six mutant P4-P6 RNAs were measured and found to be similar to that of the wild-type RNA, in spite of significant thermodynamic destabilization or stabilization. The ratios of the kinetic and thermodynamic free energy changes $\Phi = \Delta\Delta G^\ddagger/\Delta\Delta G^\circ$ are ≈0, implying a folding transition state in which most of the native-state tertiary contacts are not yet formed (an early folding transition state). The k_{obs} depends on the Mg²⁺ concentration, and the initial slope of k_{obs} versus [Mg²⁺] suggests that only ~1 Mg²⁺ ion is bound in the rate-limiting folding step. This is consistent with an early folding transition state, because folded P4-P6 binds many Mg²⁺ ions. The observation of a substantial ΔG^\ddagger despite an early folding transition state suggests that a simple two-state folding diagram for Mg²⁺-induced P4-P6 folding is incomplete. Our kinetic data are some of the first to provide quantitative values for an activation barrier and location of a transition state for tertiary folding of an RNA domain.

Keywords: activation energy; fluorescence; mutant; phi value; pyrene; tertiary folding

INTRODUCTION

A major goal of current biomolecular structural studies is a full description of folding energy landscapes. Significant effort has been dedicated to investigating protein-folding landscapes at the level of both theory (Leopold et al., 1992; Bryngelson et al., 1995; Onuchic et al., 1996, 1997; Dill & Chan, 1997; Lazaridis & Karplus, 1997; Socci et al., 1998; Dobson & Karplus, 1999) and experiment (Jackson & Fersht, 1991a, 1991b; Fersht et al., 1992; Otzen et al., 1994; Fersht, 1997; Dobson & Karplus, 1999). Experimental studies on RNA folding have also begun to reveal the overall features

of RNA-folding landscapes (Zarrinkar & Williamson, 1994; Zarrinkar et al., 1996; Pan & Sosnick, 1997; Maglott et al., 1998; Scavi et al., 1998; Treiber et al., 1998; Fang et al., 1999a, 1999b; Maglott et al., 1999; Pan et al., 2000), but little quantitative data is available.

Here we investigate tertiary folding of the P4-P6 domain of the *Tetrahymena* group I intron RNA (Murphy & Cech, 1993; Cate et al., 1996). This 160-nt RNA is substantially larger than tRNA (~75 nt), arguably the class of RNA for which folding pathways have been studied most extensively (Cantor & Schimmel, 1980). P4-P6 is large enough to possess a substantial interior surface that is relatively solvent inaccessible, the first crystallographically determined RNA structure to exemplify this feature (Cate et al., 1996). However, P4-P6 is not so large that multidomain interactions control its folding pathway. Therefore, studying P4-P6 folding allows us to quantify a global, tertiary folding process that is not dominated by kinetic traps (Thirumalai & Woodson, 1996; Pan & Sosnick, 1997; Rook et al.,

Reprint requests to: Scott K. Silverman, Department of Chemistry, 140 Roger Adams Laboratory, Box 57-5, University of Illinois at Urbana-Champaign, Urbana, Illinois 61801, USA; or Thomas R. Cech, Department of Chemistry and Biochemistry, Campus Box 215, University of Colorado at Boulder, Boulder, Colorado 80309-0215, USA.

³Current address: Department of Chemistry, 140 Roger Adams Laboratory, Box 57-5, University of Illinois at Urbana-Champaign, Urbana, Illinois 61801, USA; e-mail: scott@scs.uiuc.edu.

1998; Treiber & Williamson, 1999), for which unfolding of misfolded domains controls the overall folding.

We have described site-specific pyrene labeling of P4-P6 RNA to monitor equilibrium formation of tertiary structure (Silverman & Cech, 1999b), and we recently extended these studies to the kinetic domain with stopped-flow fluorescence (Silverman et al., 2000). In protein-folding studies, information about the folding transition state is gleaned through mutations that affect both the kinetics and thermodynamics of folding. Mutants are characterized by their values of $\Phi = \Delta\Delta G^\ddagger / \Delta\Delta G^{\circ'}$, which compare the free-energy contributions of certain residues or functional groups to the kinetic activation barrier ΔG^\ddagger and to the thermodynamic folding free energy $\Delta G^{\circ'}$ (Fersht et al., 1992; Serrano et al., 1992; Fersht, 1995; Nymeyer et al., 2000). The Φ value ($0 \leq \Phi \leq 1$) describes the location of the rate-limiting transition state along the folding reaction coordinate. A low $\Phi \approx 0$ implies an early folding transition state, one which resembles the unfolded state of the molecule. Conversely, a high $\Phi \approx 1$ indicates a late folding transition state, one that resembles the fully folded structure. Here, folding rates of mutant and wild-type P4-P6 RNAs reveal two fundamental features of the P4-P6 tertiary folding pathway: the height of the folding activation barrier and the location of the tertiary folding transition state. Our observations suggest that a simple two-state model for P4-P6 tertiary folding is incomplete.

RESULTS AND DISCUSSION

Activation free energy for P4-P6 tertiary folding

When MgCl_2 was titrated into a solution of pyrene-labeled P4-P6 in Tris-borate buffer ($1 \times \text{TB}$) at 35°C , the fluorescence intensity increased substantially, as reported earlier (Silverman & Cech, 1999b). The $[\text{Mg}^{2+}]_{1/2}$ for the major component of fluorescence change was ~ 1.1 mM (filled circles in Fig. 1). We examined the folding kinetics by mixing pyrene-labeled P4-P6 with Mg^{2+} in stopped-flow experiments as recently described (Silverman et al., 2000). Upon mixing to a final $[\text{Mg}^{2+}] = 10 \times [\text{Mg}^{2+}]_{1/2} = 10.6$ mM in $1 \times \text{TB}$ at 35°C , the major ($\sim 95\%$) component of fluorescence change occurred with $k_{\text{obs}} = 31 \text{ s}^{-1}$ ($t_{1/2} = 22$ ms; Fig. 2). When 200 mM NaCl was included in the buffer, $k_{\text{obs}} = 15 \text{ s}^{-1}$ ($t_{1/2} = 45$ ms) (Silverman et al., 2000); that is, inclusion of 200 mM Na^+ affected the folding rate only twofold.

These values of k_{obs} may be used to calculate the activation free energy ΔG^\ddagger for Mg^{2+} -induced P4-P6 tertiary folding. Assuming that the simple Eyring equation $k_{\text{obs}} = (k_B T/h) \cdot \exp(-\Delta G^\ddagger/k_B T)$ (where k_B is the Boltzmann constant and h is the Planck constant) holds, these folding rates correspond to $\Delta G^\ddagger \approx 16$ kcal/mol.

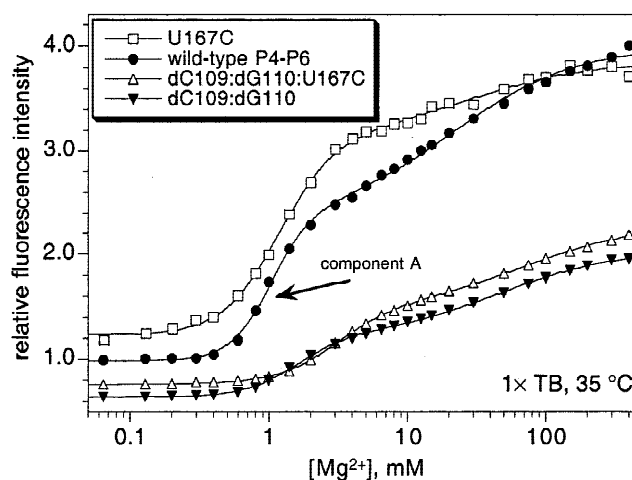


FIGURE 1. Equilibrium fluorescence titration data for pyrene-labeled P4-P6 and several destabilized mutants in Tris-borate buffer. See Silverman and Cech (1999b) for a detailed description of the experiment. The major component of fluorescence change (component A) for wild-type pyrene-labeled P4-P6 is indicated. The $[\text{Mg}^{2+}]_{1/2,A}$ values were determined for each P4-P6 RNA as follows: wild-type: 1.06 ± 0.02 mM ($n = 3$; error = S.E.M.); $\Delta\text{C}209$: 0.71 ± 0.05 mM ($n = 2$); U168C:U177G: 1.24 ± 0.05 mM ($n = 2$); dC109:dG110: 1.54 mM ($n = 1$); U167C: 2.24 ± 0.16 mM ($n = 2$); G174A: 2.45 ± 0.18 mM ($n = 2$); and dC109:dG110:U167C: 3.01 mM ($n = 1$). In titrations of mutants containing the dC109:dG110 2'-deoxy substitutions, tiny amounts of Mg^{2+} (<0.1 mM) led to a significant initial decrease (up to 40%) in the relative fluorescence intensity that was not observed with the other mutants. This may be related to the close proximity of the 2'-deoxy substitutions at C109/G110 and the pyrene chromophore at the 2'-position of U107.

The twofold difference in k_{obs} is equivalent to a shift in ΔG^\ddagger of only 0.4 kcal/mol. However, the pre-exponential term $k_B T/h$, which applies to gas-phase reactions of small molecules, is almost certainly inappropriate for more complex reactions (Kramers, 1940) such as the folding of large protein or RNA molecules in aqueous solution (Dill & Chan, 1997). Indeed, the correct pre-exponential term is probably many orders of magnitude smaller, which affects the quantitative value of ΔG^\ddagger . For example, if the pre-exponential term is lower than $k_B T/h$ by a factor of 10^6 , as would be required to shift the term from the ps^{-1} to the μs^{-1} range (Cohen & Cech, 1997), then ΔG^\ddagger is ~ 8 instead of ~ 16 kcal/mol. Experiments to determine the pre-exponential term for P4-P6 folding—or folding of any RNA—have not yet been performed. Whatever the correct term, these values of ΔG^\ddagger are at least as large as the actual (not standard) tertiary folding free energy $\Delta G'$, which is only a few kilocalories per mole at several millimolar Mg^{2+} for other large RNAs (Fang et al., 1999b) as well as for P4-P6. Thus, the activation free-energy barrier to P4-P6 tertiary folding is substantial. Previously, we studied the temperature dependence of wild-type P4-P6 folding kinetics, which allowed the separation of enthalpic and entropic contributions (Silverman et al., 2000). We found that ΔH^\ddagger and ΔS^\ddagger are both large and positive, so that the folding barrier is primarily enthalpic in origin.

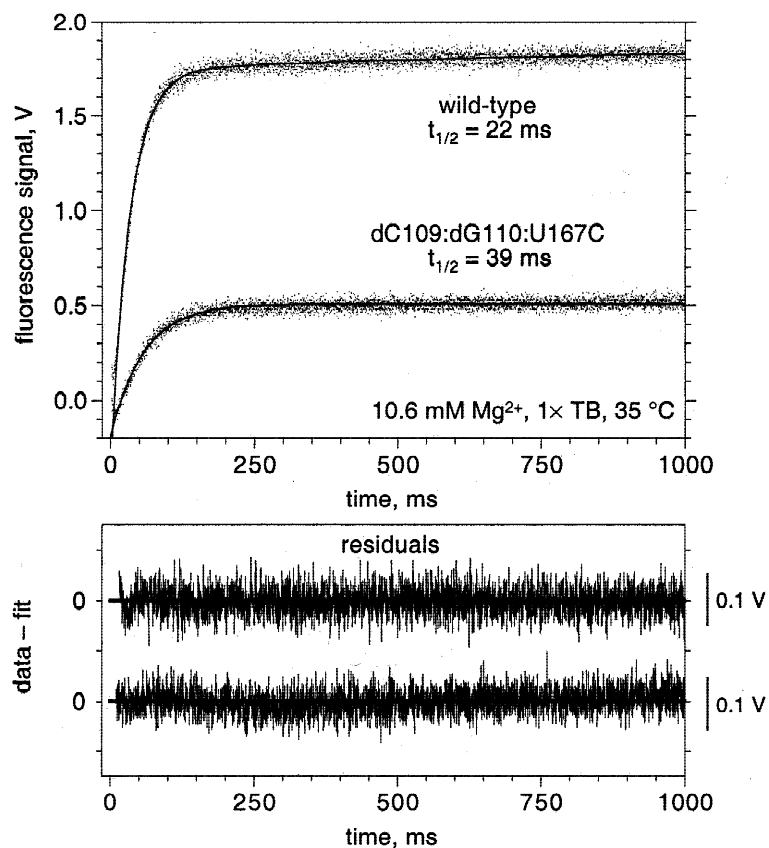


FIGURE 2. Fluorescence kinetics traces for Mg^{2+} -induced folding of pyrene-labeled P4-P6. Top trace: wild-type P4-P6. Bottom trace: thermodynamically destabilized dC109:dG110:U167C mutant. Data were collected at 35 °C immediately after 1:1 mixing of $\sim 8 \mu\text{M}$ P4-P6 in 1 \times TB buffer (annealed at 90 °C in the presence of 0.1 mM EDTA) with 21.2 mM MgCl_2 in 1 \times TB, providing final concentrations of $\sim 4 \mu\text{M}$ RNA and 10.6 mM MgCl_2 . The instrument dead time was 1.3 ms. For each trace, six shots (each 4,000 data points at intervals of 0.25 ms) were averaged. Increasing voltage corresponds to increasing fluorescence intensity. Data from 10–1,000 ms of the top trace were fit with a double exponential with a major (94% of fluorescence change) component $k_{obs} = 31.0 \pm 0.2 \text{ s}^{-1}$ ($t_{1/2} = 22.4 \pm 0.2 \text{ ms}$) and a minor (6%) component $k_{obs} = 1.29 \pm 0.07 \text{ s}^{-1}$ ($t_{1/2} = 0.54 \pm 0.03 \text{ s}$). Data from 10–1,000 ms of the bottom trace were fit with a single exponential with $k_{obs} = 17.7 \pm 0.1 \text{ s}^{-1}$ ($t_{1/2} = 39.2 \pm 0.2 \text{ ms}$). In both cases, additional traces recorded from the same samples out to 20 s showed no further kinetic components (data not shown). Data analogous to that shown in the top trace obtained at very high $[\text{Mg}^{2+}] = 318 \text{ mM}$ ($= 300 \times [\text{Mg}^{2+}]_{1/2}$) showed a minor ($\sim 10\%$) *decreasing* fluorescence component with $t_{1/2} \sim 3 \text{ s}$ (data not shown); such a decreasing component was not observed at lower $[\text{Mg}^{2+}]$. The lower apparent fluorescence change for the destabilized mutant compared to wild type is accounted for by the drop in fluorescence at extremely low $[\text{Mg}^{2+}]$ observed only for the mutant (Fig. 1).

Minor kinetic effects of mutations indicate an early P4-P6 folding transition state

In several previous studies (Juneau & Cech, 1999; Silverman & Cech, 1999a, 1999b; Silverman et al., 1999), we identified site-directed mutations and specific 2'-deoxy substitutions that substantially affect the P4-P6 thermodynamic tertiary folding free energy ΔG° . Here we explore the relationship between P4-P6 folding kinetics and thermodynamic stability by examining the effects of these mutations and substitutions on the P4-P6 tertiary folding rate. Kinetic data (k_{obs}) for folding of wild-type P4-P6 and six mutants are shown as a function of $[\text{Mg}^{2+}]$ in Figure 3. Overall, there is very little difference between the folding rate of any mutant and of wild-type P4-P6 at any given $[\text{Mg}^{2+}]$. In particular, the data for wild-type P4-P6 and three mutants all obtained at 10.6 mM Mg^{2+} (arrow in Fig. 3) show a difference in folding rates of less than a factor of two: $k_{obs} = 31 \text{ s}^{-1}$ ($t_{1/2} = 22 \text{ ms}$) for wild-type P4-P6, and $k_{obs} = 18 \text{ s}^{-1}$ ($t_{1/2} = 39 \text{ ms}$) for the dC109:dG110:U167C mutant (Fig. 2). This corresponds to a difference in activation free energies $\Delta\Delta G^\ddagger$ of $< 0.4 \text{ kcal/mol}$, independent of the Eyring pre-exponential term, which cancels in computing $\Delta\Delta G^\ddagger$. In contrast, the thermodynamic destabilizations for these mutants are quite large. In the case of the dC109:dG110:U167C triple mutant, which has two 2'-deoxy substitutions at C109 and G110

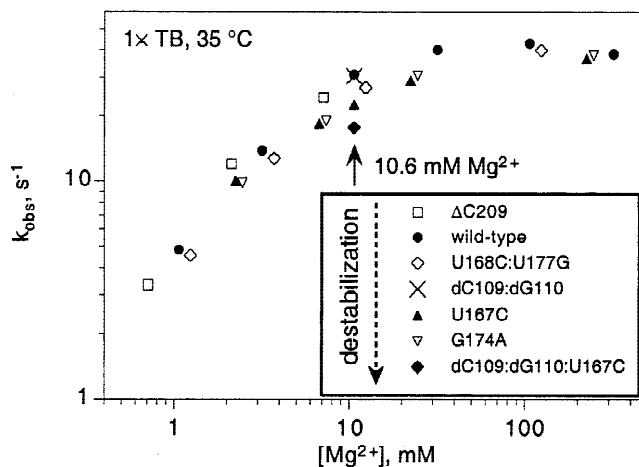


FIGURE 3. Dependence of the Mg^{2+} -induced folding rate of P4-P6 on $[\text{Mg}^{2+}]$ and on mutations that alter the tertiary folding energy ΔG° of P4-P6. Data are shown for wild-type P4-P6 (filled circles) and for six mutants (other symbols). Data were collected in 1 \times TB buffer at 35 °C as described in the Figure 2 legend. The $\Delta\text{C}209$ mutation stabilizes P4-P6 tertiary folding by $\sim 1.1 \text{ kcal/mol}$, whereas all of the other mutations destabilize folding by varying amounts ($\geq 3 \text{ kcal/mol}$ for the dC109:dG110:U167C mutant), as described in Materials and Methods. Kinetic data for wild-type P4-P6 and the site-directed (non-2'-deoxy) mutants were obtained at 1, 3, 10, 30, 100, or 300 times the $[\text{Mg}^{2+}]_{1/2}$ value for the particular RNA. The amplitude of fluorescence change was very small when $[\text{Mg}^{2+}] < [\text{Mg}^{2+}]_{1/2}$, making it difficult to determine k_{obs} values accurately. Data for the two 2'-deoxy mutants were obtained only at 10.6 mM, which is $10 \times [\text{Mg}^{2+}]_{1/2}$ for wild-type pyrene-labeled P4-P6 and $\sim 3 \times [\text{Mg}^{2+}]_{1/2}$ for the most destabilized dC109:dG110:U167C mutant (Fig. 1).

in addition to the U167C mutation, the 2'-deoxy substitutions together are destabilizing by $\Delta\Delta G^{\circ'} = 1.5$ kcal/mol (Silverman & Cech, 1999a), and the U167C point mutation is destabilizing by at least the same amount and possibly several kilocalories per mole more (Silverman et al., 1999), for a total estimated destabilization of $\Delta\Delta G^{\circ'} = 3$ kcal/mol.

These kinetic data indicate that very little of the $\Delta\Delta G^{\circ'}$ for any given P4-P6 mutant is felt in the rate-limiting folding transition state. The ratio $\Phi = \Delta\Delta G^{\ddagger}/\Delta\Delta G^{\circ'}$ is very small; the significantly destabilized dC109:dG110 double mutant has k_{obs} approximately equal to that of wild-type P4-P6, implying $\Phi \approx 0$. This low value of Φ indicates an early transition state for the rate-determining step of Mg^{2+} -induced P4-P6 tertiary folding.

A folding energy diagram for P4-P6

Our kinetic data may be related to an energy diagram for P4-P6 tertiary folding. Consider a very simple diagram in which the unfolded state U (which has only secondary structure) folds into the folded state F (with both secondary and tertiary structure) through a single transition state \ddagger (Fig. 4). An early transition state for P4-P6 folding is consistent with the Hammond postulate (Hammond, 1955; Matouschek & Fersht, 1993;

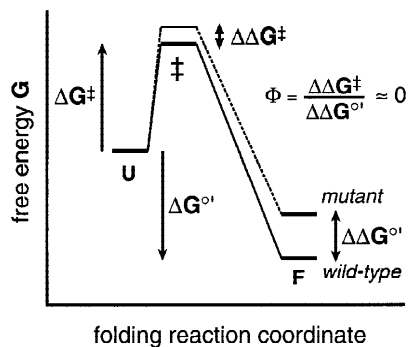


FIGURE 4. A simple two-state energy diagram for P4-P6 tertiary folding. A single transition state (\ddagger) is located between unfolded (U; secondary structure only) and folded (F; secondary plus tertiary structure) states. The dual observations of a large ΔG^{\ddagger} and an early transition state (low Φ) suggest that this model is incomplete. The folding reaction coordinate (or “order parameter” (Socci et al., 1998)) is not well defined, as the structure of P4-P6 at any point along the folding pathway other than the fully folded state (Cate et al., 1996) is not known with precision. The free energy of the folded state is shown as lower than that of the unfolded state (i.e., $\Delta G' < 0$), which is the case at $[Mg^{2+}] \gg [Mg^{2+}]_{1/2}$ (e.g., 10.6 mM Mg^{2+} in Tris-borate buffer at 35°C). The activation barrier ΔG^{\ddagger} is ~ 8 –16 kcal/mol depending on the Eyring pre-exponential term as described in the text. The value of $\Phi = \Delta\Delta G^{\ddagger}/\Delta\Delta G^{\circ'} \approx 0$ was determined from the folding kinetics of several mutant P4-P6 RNAs (Fig. 3). The free energy profile of a generic, destabilized mutant RNA is shown; the magnitude of $\Delta\Delta G^{\ddagger}$ relative to $\Delta\Delta G^{\circ'}$ is exaggerated for clarity. The energy of the unfolded state is depicted as unperturbed by a mutation that affects $\Delta G^{\circ'}$, which is equivalent to the assumption that the tested mutations specifically affect interactions only in the folded state of P4-P6.

Matouschek et al., 1995), because Mg^{2+} -induced P4-P6 folding is “downhill” in free energy ($\Delta G^{\circ'} < 0$, and $\Delta G' < 0$ under the experimental conditions). The observation of a very low Φ value indicates that the transition state \ddagger strongly resembles the unfolded state U. That is, most of the tertiary contacts that specifically stabilize the fully folded state F are not yet formed at \ddagger .

However, the dual observations of low Φ and large ΔG^{\ddagger} prompt a question: if \ddagger resembles U, then why is ΔG^{\ddagger} so large? Some interactions must be disrupted to explain the substantial folding barrier. The existence of structure in “unfolded” tRNA was recognized long ago (Fresco et al., 1966), even before high-resolution tRNA structures were known. However, we know little about the structure of unfolded RNA molecules like P4-P6, and it is unclear what sorts of interactions must be disrupted to distort the RNA conformation from U to \ddagger (a similar issue has been pointed out for proteins (Ny-meyer et al., 2000)). Such interactions in P4-P6 could be nonnative tertiary contacts in the Mg^{2+} -free unfolded state (Deras et al., 2000; Silverman et al., 2000), or stacking interactions in the “hinge” region that connects the quasihelical halves of P4-P6 (Murphy & Cech, 1993; Cate et al., 1996; Szewczak & Cech, 1997). There is some secondary structure rearrangement accompanying the tertiary folding of P4-P6 (Wu & Tinoco, 1998; Silverman et al., 1999), and this could also contribute to the activation barrier. Whatever the disrupted structural interactions, a large ΔG^{\ddagger} seems inconsistent with a low value of Φ , because the former implies a substantial difference between U and \ddagger , whereas the latter suggests that U and \ddagger have similar structures. We therefore propose that the simple two-state diagram of Figure 4 is an incomplete description of Mg^{2+} -induced P4-P6 tertiary folding.

Application of Φ -value analysis to a non-two-state folding or unfolding process is reasonable (Serrano et al., 1992), but care must be taken in the interpretation of the data. In the present case, the low value $\Phi \approx 0$, taken alone, implies only that most of the native-state tertiary contacts are not yet formed at the rate-determining folding transition state. A more accurate folding diagram to replace Figure 4 would require more direct data on the nature of any intermediate(s) along the folding pathway.

Mechanistic role of Mg^{2+} in the folding process

Because P4-P6 tertiary folding incorporates at least five Mg^{2+} ions (Cate et al., 1997), one might expect that the folding kinetics would depend strongly on $[Mg^{2+}]$. Indeed, as the Mg^{2+} concentration was raised in the range of 1–30 mM, where ~ 1 mM is $[Mg^{2+}]_{1/2}$ for wild-type P4-P6, k_{obs} increased significantly (Fig. 3, filled circles), but the slope was only ~ 1 (or a little less). However, above ~ 30 mM Mg^{2+} ($\sim 30 \times [Mg^{2+}]_{1/2}$ for

wild-type P4-P6), the rate leveled off with further increases in $[Mg^{2+}]$.

These data help to reveal the role of Mg^{2+} in the RNA folding process. For $[Mg^{2+}] > 30$ mM, folding is not rate limited by Mg^{2+} binding but must instead be limited by conformational changes occurring subsequent to Mg^{2+} binding. However, for $[Mg^{2+}] < 30$ mM, the rate-limiting folding step involves chelation of only ~ 1 Mg^{2+} ion. This observation is consistent with an early folding transition state as follows. Formation of tertiary interactions in the fully folded state presumably requires incorporation of numerous Mg^{2+} ions into specific binding sites (Cate et al., 1997). However, because most of these tertiary interactions are not yet formed at the rate-determining folding transition state, one would expect far fewer Mg^{2+} ions to be required to achieve this transition state, and indeed only ~ 1 such ion is required. For folding of the 112-nt *Escherichia coli* α mRNA pseudoknot, the rate-limiting conformational change was also reported to involve binding of only a single Mg^{2+} ion (Gluick et al., 1997).

CONCLUSIONS

We report some of the first quantitative values for an activation barrier and location of the transition state for tertiary folding of an RNA domain (Maglott et al., 1999). Upon mixing with Mg^{2+} at 35 °C, P4-P6 folds with $k_{obs} = 15\text{--}31$ s⁻¹ ($t_{1/2} \approx 20\text{--}50$ ms), equivalent to an activation free energy ΔG^\ddagger of $\sim 8\text{--}16$ kcal/mol. Further experiments are required to calibrate more precisely the relationship between k_{obs} and ΔG^\ddagger for all RNAs, including P4-P6. By examining the folding rates of thermodynamically perturbed P4-P6 mutants, we demonstrate an early transition state for P4-P6 tertiary folding. That is, most of the native tertiary contacts in P4-P6 are not yet formed at the rate-determining transition state for Mg^{2+} -induced folding. We also find that only ~ 1 Mg^{2+} ion is involved in the rate-determining folding step at low $[Mg^{2+}]$. These observations suggest that the energy diagram for P4-P6 tertiary folding involves more than two states.

MATERIALS AND METHODS

RNA preparation

RNAs were prepared as described elsewhere (Silverman et al., 2000), by ligation of pyrene-labeled 15-mer oligonucleotides to T7 RNA polymerase transcripts comprising the remainder of P4-P6 ($\Delta 15$ -P4-P6 transcripts) (Silverman & Cech, 1999b). The pyrene was site-specifically incorporated at the 2' position of U107. All oligonucleotides were prepared at Dharmacon Research, Inc. (Boulder, CO) and purified by PAGE. RNAs containing the destabilizing ($\Delta\Delta G^{o'} = 1.5$ kcal/mol) dC109:dG110 double-2'-deoxy substitutions (Silverman & Cech, 1999a) were prepared using 15-mer oligonucleotides synthe-

sized using the appropriate 2'-deoxyphosphoramidites. The $\Delta C209$ deletion stabilizes folding of P4-P6 (Juneau & Cech, 1999) by 1.1 kcal/mol, determined by non-denaturing gels as described (Silverman & Cech, 1999a; K. Juneau and T.R. Cech, unpubl.). The destabilizing U168C:U177G double mutation was identified during the course of a previous study (Silverman et al., 1999) as causing a small shift in the Mg^{2+} dependence of P4-P6 folding; from non-denaturing gel data (Silverman & Cech, 1999a), the estimated $\Delta\Delta G^{o'}$ at 35 °C is 0.4 kcal/mol (data not shown). The destabilizing (1.5–6 kcal/mol) U167C and G174A mutations were described previously (Silverman & Cech, 1999b; Silverman et al., 1999). RNAs containing the $\Delta C209$, U168C:U177G, U167C, or G174A mutations were obtained using $\Delta 15$ -P4-P6 transcripts prepared from appropriately mutated DNA templates.

Equilibrium and stopped-flow fluorescence measurements

Fluorescence experiments were performed as described elsewhere (Silverman et al., 2000). The $1\times$ TB buffer is 89 mM each Tris and boric acid, pH 8.3.

ACKNOWLEDGMENTS

We thank Susy Kohout for help with maintaining the stopped-flow fluorescence spectrometer and Martin Gruebele, Sarah Woodson, Mike Deras, and Gary Glick for helpful discussions. This work was supported by grant GM28039 from the National Institutes of Health to T.R.C. S.K.S. was supported by an American Cancer Society postdoctoral fellowship and was a fellow of the Helen Hay Whitney Foundation. T.R.C. is an American Cancer Society Professor. We thank the W.M. Keck foundation for generous support of the Program in Molecular and Cellular Structure on the Boulder campus.

Received August 24, 2000; returned for revision October 13, 2000; revised manuscript received October 30, 2000

REFERENCES

- Bryngelson JD, Onuchic JN, Socci ND, Wolynes PG. 1995. Funnels, pathways, and the energy landscape of protein folding: A synthesis. *Proteins* 21:167–195.
- Cantor CR, Schimmel PR. 1980. *Biophysical chemistry*, Vol. III. San Francisco: W.H. Freeman and Company.
- Cate JH, Gooding AR, Podell E, Zhou K, Golden BL, Kundrot CE, Cech TR, Doudna JA. 1996. Crystal structure of a group I ribozyme domain: Principles of RNA packing. *Science* 273:1678–1685.
- Cate JH, Hanna RL, Doudna JA. 1997. A magnesium ion core at the heart of a ribozyme domain. *Nat Struct Biol* 4:553–558.
- Cohen SB, Cech TR. 1997. Dynamics of Thermal motions within a large catalytic RNA investigated by cross-linking with thiol-disulfide interchange. *J Am Chem Soc* 119:6259–6268.
- Deras ML, Brenowitz M, Ralston CY, Chance MR, Woodson SA. 2000. Folding mechanism of the *Tetrahymena* ribozyme P4-P6 domain. *Biochemistry* 39:10975–10985.
- Dill KA, Chan HS. 1997. From Levinthal to pathways to funnels. *Nat Struct Biol* 4:10–19.
- Dobson CM, Karplus M. 1999. The fundamentals of protein folding: Bringing together theory and experiment. *Curr Opin Struct Biol* 9:92–101.
- Fang X, Pan T, Sosnick TR. 1999a. Mg^{2+} -dependent folding of a large ribozyme without kinetic traps. *Nat Struct Biol* 6:1091–1095.

- Fang X, Pan T, Sosnick TR. 1999b. A thermodynamic framework and cooperativity in the tertiary folding of a Mg²⁺-dependent ribozyme. *Biochemistry* 38:16840–16846.
- Fersht AR. 1995. Characterizing transition states in protein folding: An essential step in the puzzle. *Curr Opin Struct Biol* 5:79–84.
- Fersht AR. 1997. Nucleation mechanisms in protein folding. *Curr Opin Struct Biol* 7:3–9.
- Fersht AR, Matouschek A, Serrano L. 1992. The folding of an enzyme. I. Theory of protein engineering analysis of stability and pathway of protein folding. *J Mol Biol* 224:771–782.
- Fresco JR, Adams A, Ascione R, Henley D, Lindahl T. 1966. Tertiary structure in transfer ribonucleic acids. *Cold Spring Harbor Symp Quant Biol* 31:527–537.
- Gluick TC, Gerstner RB, Draper DE. 1997. Effects of Mg²⁺, K⁺, and H⁺ on an equilibrium between alternate conformations of an RNA pseudoknot. *J Mol Biol* 270:451–463.
- Hammond GS. 1955. A correlation of reaction rates. *J Am Chem Soc* 77:334–338.
- Jackson SE, Fersht AR. 1991a. Folding of chymotrypsin inhibitor-2. 1. Evidence for a two-state transition. *Biochemistry* 30:10428–10435.
- Jackson SE, Fersht AR. 1991b. Folding of chymotrypsin inhibitor-2. 2. Influence of proline isomerization on the folding kinetics and thermodynamic characterization of the transition state of folding. *Biochemistry* 30:10436–10443.
- Juneau K, Cech TR. 1999. In vitro selection of RNAs with increased tertiary structure stability. *RNA* 5:1119–1129.
- Kramers HA. 1940. Brownian motion in a field of force and the diffusion model of chemical reactions. *Physica* 7:284–304.
- Lazaridis T, Karplus M. 1997. “New view” of protein folding reconciled with the old through multiple unfolding simulations. *Science* 278:1928–1931.
- Leopold PE, Montal M, Onuchic JN. 1992. Protein folding funnels: A kinetic approach to the sequence-structure relationship. *Proc Natl Acad Sci USA* 89:8721–8725.
- Maglott EJ, Deo SS, Przykorska A, Glick GD. 1998. Conformational transitions of an unmodified tRNA: Implications for RNA folding. *Biochemistry* 37:16349–16359.
- Maglott EJ, Goodwin JT, Glick GD. 1999. Probing the structure of an RNA tertiary unfolding transition state. *J Am Chem Soc* 121:7461–7462.
- Matouschek A, Fersht AR. 1993. Application of physical organic chemistry to engineered mutants of proteins: Hammond postulate behavior in the transition state of protein folding. *Proc Natl Acad Sci USA* 90:7814–7818.
- Matouschek A, Otzen DE, Itzhaki LS, Jackson SE, Fersht AR. 1995. Movement of the position of the transition state in protein folding. *Biochemistry* 34:13656–13662.
- Murphy FL, Cech TR. 1993. An independently folding domain of RNA tertiary structure within the *Tetrahymena* ribozyme. *Biochemistry* 32:5291–5300.
- Nymeyer H, Socci ND, Onuchic JN. 2000. Landscape approaches for determining the ensemble of folding transition states: Success and failure hinge on the degree of frustration. *Proc Natl Acad Sci USA* 97:634–639.
- Onuchic JN, Luthey-Schulten Z, Wolynes PG. 1997. Theory of protein folding: The energy landscape perspective. *Annu Rev Phys Chem* 48:545–600.
- Onuchic JN, Socci ND, Luthey-Schulten Z, Wolynes PG. 1996. Protein folding funnels: The nature of the transition state ensemble. *Fold Des* 1:441–450.
- Otzen DE, Itzhaki LS, Elmasry NF, Jackson SE, Fersht AR. 1994. Structure of the transition state for the folding/unfolding of the barley chymotrypsin inhibitor 2 and its implications for mechanisms of protein folding. *Proc Natl Acad Sci USA* 91:10422–10425.
- Pan J, Deras ML, Woodson SA. 2000. Fast folding of a ribozyme by stabilizing core interactions: Evidence for multiple folding pathways in RNA. *J Mol Biol* 296:133–144.
- Pan T, Sosnick TR. 1997. Intermediates and kinetic traps in the folding of a large ribozyme revealed by circular dichroism and UV absorbance spectroscopies and catalytic activity. *Nat Struct Biol* 4:931–938.
- Rook MS, Treiber DK, Williamson JR. 1998. Fast folding mutants of the *Tetrahymena* group I ribozyme reveal a rugged folding energy landscape. *J Mol Biol* 281:609–620.
- Sclavi B, Sullivan M, Chance MR, Brenowitz M, Woodson SA. 1998. RNA folding at millisecond intervals by synchrotron hydroxyl radical footprinting. *Science* 279:1940–1943.
- Serrano L, Matouschek A, Fersht AR. 1992. The folding of an enzyme. III. Structure of the transition state for unfolding of barnase analyzed by a protein engineering procedure. *J Mol Biol* 224:805–818.
- Silverman SK, Cech TR. 1999a. Energetics and cooperativity of tertiary hydrogen bonds in RNA structure. *Biochemistry* 38:8691–8702.
- Silverman SK, Cech TR. 1999b. RNA tertiary folding monitored by fluorescence of covalently incorporated pyrene. *Biochemistry* 38:14224–14237.
- Silverman SK, Deras ML, Woodson SA, Scaringe SA, Cech TR. 2000. Multiple folding pathways for the P4-P6 RNA domain. *Biochemistry* 39:12465–12475.
- Silverman SK, Zheng M, Wu M, Tinoco I Jr, Cech TR. 1999. Quantifying the energetic interplay of RNA tertiary and secondary structure interactions. *RNA* 5:1665–1674.
- Socci ND, Onuchic JN, Wolynes PG. 1998. Protein folding mechanisms and the multidimensional folding funnel. *Proteins* 32:136–158.
- Szewczak AA, Cech TR. 1997. An RNA internal loop acts as a hinge to facilitate ribozyme folding and catalysis. *RNA* 3:838–849.
- Thirumalai D, Woodson SA. 1996. Kinetics of folding of proteins and RNA. *Acc Chem Res* 29:433–439.
- Treiber DK, Rook MS, Zarrinkar PP, Williamson JR. 1998. Kinetic intermediates trapped by native interactions in RNA folding. *Science* 279:1943–1946.
- Treiber DK, Williamson JR. 1999. Exposing the kinetic traps in RNA folding. *Curr Opin Struct Biol* 9:339–345.
- Wu M, Tinoco I Jr. 1998. RNA folding causes secondary structure rearrangement. *Proc Natl Acad Sci USA* 95:11555–11560.
- Zarrinkar PP, Wang J, Williamson JR. 1996. Slow folding kinetics of RNase P RNA. *RNA* 2:564–573.
- Zarrinkar PP, Williamson JR. 1994. Kinetic intermediates in RNA folding. *Science* 265:918–924.